Published in final edited form as:
Chem Res Toxicol. 2007 September ; 20(9): 1331–1341.

Metabolism of Benzo[*a*]pyrene in Human Bronchoalveolar H358 Cells Using Liquid Chromatography-Mass Spectrometry

Hao Jiang[†], **Stacy L. Gelhaus**[‡], **Dipti Mangal**[‡], **Ronald G. Harvey**[§], **Ian A. Blair**[‡], and **Trevor M. Penning**[†,*]

†*Centers of Excellence in Environmental Toxicology, University of Pennsylvania School of Medicine, Philadelphia, PA 19104-6084*

‡*Cancer Pharmacology, Department of Pharmacology, University of Pennsylvania School of Medicine, Philadelphia, PA 19104-6084*

§*The Ben May Institute for Cancer Research, University of Chicago, Chicago, IL 60637*

Abstract

Benzo[*a*]pyrene (B[*a*]P), a representative polycyclic aromatic hydrocarbon (PAH), is metabolically activated by three enzymatic pathways; by peroxidases (e.g. cytochrome P450-peroxidase) to yield radical cations; by P4501A1/1B1 monoxygenation plus epoxide hydrolase to yield diol-epoxides; and by P4501A1/1B1 monoxygenation, epoxide hydrolase plus aldo-keto reductases (AKRs) to yield *o*-quinones. In humans, a major exposure site for environmental and tobacco smoke PAH is the lung, however, the profile of B[*a*]P metabolites formed at this site has not been well characterized. In this study, human bronchoalveolar H358 cells were exposed to B[*a*]P, and metabolites generated by peroxidase (B[*a*]P-1,6- and B[*a*]P-3,6-diones), from cytochrome P4501A1/1B1 monooxygenation (3-hydroxyl-B[*a*]P, B[*a*]P-7,8- and 9,10-*trans*-dihydrodiols, and B[*a*]P -*r*-7,*t*-8,*t*-9,*c*-10-tetrahydrotetrol (B[*a*]P -tetrol-1)), and from AKRs (B[*a*]P-7,8-dione) were detected and quantified by RP-HPLC-with in line photo-diode array and radiometric detection, and identified by LC-MS. Progress curves showed a lag-phase in the formation of 3-hydroxy-B[*a*]P, B[*a*]P-7,8-*trans*-dihydrodiol, B[*a*]P-tetraol-1 and B[*a*]P-7,8-dione over 24 h. Northern blot analysis showed that B [*a*]P induced P4501B1 and AKR1C isoforms in H358 cells in a time-dependent manner providing an explanation for the lag-phase. Pretreatment of H358 cells with 10 nM 2,3,7,8-tetrachlorodibenzo-*p*-dioxin, (TCDD) eliminated this lag-phase, but did not alter the levels of the individual metabolites observed, suggesting that both B[*a*]P and TCDD induction ultimately yield the same B[*a*]P-metabolic profile. The one exception was B[*a*]P-3,6-dione which was formed without a lag-phase in the absence and presence of TCDD, suggesting that the peroxidase responsible for its formation was neither P4501A1 nor 1B1. Candidate peroxidases that remain include PGH synthases and uninduced P450 isoforms. This study shows that the P4501A1/1B1 and AKR pathways are inducible in human lung cells and that the peroxidase pathway was not. It also provides evidence that each of the pathways of PAH-activation yield their distinctive metabolites in H358 human lung cells and that each pathway may contribute to the carcinogenic process.

Keywords

Benzo[*a*]pyrene; cytochrome P450; aldo-keto reductases; radical-cations; TCDD and monofunctional inducers

*To whom correspondence should be addressed: Dr. Trevor M. Penning. Department of Pharmacology, University of Pennsylvania School of Medicine, 130C John Morgan Building[1], 3620 Hamilton Walk, Philadelphia, PA 19104-6084. Tel:: 215-898-9445. FAX: 215-573-2236. E-mail: penning@pharm.med.upenn.edu.

Introduction

Lung cancer is the major cause of cancer death in the US adult population and 174,470 new cases are reported annually (1). Ninety percent of all lung cancer is seen in individuals who smoke suggesting that exposure to tobacco carcinogens are cuasative. Major classes of carcinogens present in cigarette smoke, include nicotine derived nitrosamino ketones, polycyclic aromatic hydrocarbons (PAH), aldehydes, butadiene, benzene and heavy metals (2-5). PAH are also ubiquitous environmental pollutants and thus PAH exposure may be a contributing factor to never-smokers with lung cancer (6-8). Remarkably, even though human lung epithelial cells are the target cells for cellular transformation, LC/MS/MS methods have not been applied to determine the metabolic fate of B[*a*]P, a representative PAH in these cells.

Three major routes of B[*a*]P metabolism are shown in Figure 1. In the presence of a peroxide, B[*a*]P can undergo one-electron oxidation at C6 by cytochrome P450 (P450) peroxidase or other peroxidases (e.g. PGH-synthase or lactoperoxidase) to generate a radical-cation (9-11). In the peroxidase cycle B[*a*]P acts as a co-reductant of the Fe^{4+}-protoporphyrin IX radical cation (Fe^{V+}) and forms a radical cation itself at C6 (12). The activated carbon can accept oxygen from the Fe^{4+}=O species to form 6-hydroxy-B[*a*]P which autooxidizes to yield B[*a*]P-1,6-, 3,6- or 6,12-diones (13). These quinones undergo one electron reduction by microsomal NADPH-cytochrome P450 reductase, microsomal NADH-cytochrome b5 reductase, or mitochondrial NADH:ubiquinone oxidoreductase (14) to yield semiquinone anion radicals which in air redox-cycle back to the diones, with the generation of ROS [peroxide (O_2^{2-}), superoxide anion ($O_2^{\cdot-}$) and hydroxyl radical ($OH^{\cdot}$)] (15).

B[*a*]P can also undergo mono-oxygenation catalyzed by the microsomal NADPH-dependent P450 isoforms (1A1 and 1B1), to yield a series of arene oxides, which can either rearrange to yield 3, 7, or 9-hydroxy-B[*a*]P or be hydrated by microsomal epoxide hydrolase (EH) to yield the corresponding B[*a*]P-7,8- or 9,10-*trans*-dihydrodiols. The non-K-region B[*a*]P-7,8-dihydrodiol is further mono-oxygenated by P4501A1/1B1 to yield the reactive *anti*-B[*a*]P-7,8-diol-9,10-epoxide (*anti*-B[*a*]PDE) (16,17) which is a rodent lung carcinogen. Formation of the diol-epoxide thus requires the combined action of P450 isoforms and EH.

B[*a*]P -7,8-dihydrodiol is also oxidized by human aldo-keto reductases (AKR1A1, 1C1-1C4) to form a ketol which spontaneously rearranges to form a catechol (18-21). The catechol is unstable and undergoes a one-electron autooxidation in air to form an *o*-semiquinone anion radical followed by a second one electron autooxidation to generate a reactive Michael acceptor, B[*a*]P-7,8-dione and ROS (22). B[*a*]P-7,8-dione can be reduced enzymatically or non-enzymatically back to the catechol establishing futile redox-cycles, that result in the generation and amplification of ROS until cellular reducing equivalents are depleted (14,23). Formation of B[*a*]P-7,8-dione thus requires the combined action of P450 isoforms, EH and AKRs.

Generation of B[*a*]P-radical-cations, B[*a*]P-diol-epoxides and B[*a*]P-*o*-quinones and ROS could each play a role in human lung carcinogenesis. For example, B[*a*]P-radical-cations generate depurinating adducts, including B[*a*]P-6-C8-Gua, B[*a*]P-6-N7-Gua and B[*a*]P-6-N7-Ade (10,11). Metabolites derived from radical cations, B[*a*]P-1,6- and B[*a*]P-3,6-dione also activate the epidermal growth factor receptor (EGFR) via the generation of hydrogen peroxide, leading to increased MCF10A cell proliferation (24) suggesting a potential role in tumor promotion.

anti-B[*a*]PDE is mutagenic in bacterial and mammalian cell assays (25) and causes pulmonary adenomas in mice (26). These properties result from the formation of stable bulky DNA adducts with 2′-deoxyguanosine (dGuo) (27,28). Furthermore, *anti*-B[*a*]PDE activates the c-H-*ras*-1 proto-oncogene to transform NIH/3T3 cells, which can be assigned to a single point mutation

in the 12th codon of *ras* (G to T transversion) (29). Reaction of *anti*-B[*a*]PDE with the *p53* tumor suppressor gene leads to adduct formation in codons 157, 158, 179, 248 and 273 (30). Mutations in these codons inactivate p53 and correspond to "hot-spots" most mutated in p53 in lung cancer patients. Thus a compelling case can be made for the role of *anti*-B[*a*]PDE in lung cancer causation.

The reactive and redox-active B[*a*]P-7,8-dione formed by AKRs can form stable hydrated N^2-dGuo and N^6-dAdo adducts as well as depurinating N7-Gua adducts (31-34). N7-Gua depurinating adducts have the potential to give rise to the G to T transversions observed in the H-*ras* gene. B[*a*]P-7,8-dione will also mutate the tumor suppressor gene *p53 in vitro* and in A549 human lung adenocarcinoma cells (35,36). *In vitro*, PAH *o*-quinones were only mutagenic under redox-cycling conditions. Mutagenicity was abolished with ROS scavengers, and the primary lesion detected was 8-oxo-dGuo (35,37,38). The point mutations most often seen were G to T transversions implicating 8-oxo-dGuo as the adduct responsible. Which of these three pathways of PAH activation dominate in human bronchial epithelial cells is unknown.

The individual peroxidases that form radical cations have not been assigned but it is anticipated that they will be P450 isoforms. In humans P450s most implicated in PAH activation are 1A1, 1B1 (39,40) and the AKRs most involved are (1A1, 1C1-1C4) (20,21,41). These enzymes are differentially expressed and regulated. P4501A1/1B1 are extra-hepatic enzymes that are inducible by PAHs and polyhalogenated hydrocarbons (TCDD, etc), via the aryl hydrocarbon receptor (AhR) (42-44). Of the five human AKR isoforms (1A1, 1C1-1C4) most involved in the metabolic activation of PAH *trans*-dihydrodiols none are directly induced by the AhR. Instead induction is achieved by electrophilic metabolites of B[*a*]P that signal to the antioxidant response element (ARE) (18,45). AKR1C1/2 are overexpressed in non-small cell lung carcinoma and may serve as indicators of poor prognosis (46). We showed that human lung adenocarcinoma A549 cells have high endogenous expression of AKR1C1-1C3 and convert PAH *trans*-dihydrodiols to PAH *o*-quinones (21). The competing roles of P4501A1/1B1 and AKR1A1 in the metabolic activation of B[*a*]P-7,8-dihydrodiol has been examined in H358 cells manipulated to express either enzyme system. We found that AKR1A1 had a dual effect: it oxidized (-)-B[*a*]P-7,8-dihydrodiol to B[*a*]P-7,8-dione, but B[*a*]P-7,8-dione also acted as a ligand for the AhR leading to the induction of the P4501B1 gene (47). Thus, the P450 pathway generates metabolites that induce the AKR pathway and vice versa.

B[*a*]P metabolism has been studied in monolayer cultures of human bronchial epithelial cells (48), primary cultures of human hepatocytes (49), mammary tumor cells (50), liver microsomes and lymphocytes (51). However, these studies were performed without an appreciation for all the participating pathways, and often without the use of appropriate analytical chemistry to identify all the metabolites. We now use human bronchoalveolar H358 cells as a model to study the metabolic profile of B[*a*]P in human lung epithelial cells. Using LC-MS based methodology we provide evidence for the presence of all three pathways of PAH activation in these cells. While the P4501A1/1B1 and AKR enzymes are inducible, peroxidase derived B[*a*]P metabolites were observed without enzyme induction. The identity of the peroxidase involved remains elusive.

Material and Methods

Caution

All PAHs are potentially hazardous and should be handled in accordance with NIH guidelines for the Use of Chemical Carcinogens.

Chemicals and Reagents

Cell culture medium and reagents were all obtained from Invitrogen Co. (Carlsbad, CA) except fetal bovine serum from (FBS) Hyclone (Logan, Utah). [G-^{3}H]-B[*a*]P (specific activity 82.0 Ci/mmol, ≥ 98% pure by HPLC) was purchased from Amersham Biosciences UK Limited (Buckinghamshire, UK). The non-radiolabeled B[*a*]P metabolite standards and TCDD were obtained from either the NCI Chemical Carcinogen Standard Reference Repository (Midwest Research Institute, Kansas City, Missouri) or they were synthesized according to published methods (52). The purity and identity of all B[*a*]P metabolites was established by LC-MS. All solvents were HPLC grade, and all other chemicals used were of the highest grade available.

Cell Culture

Transformed human bronchoalveolar H358 cells (type II, epithelial origin) were obtained from the American Type Culture Collection (ATCC #CRL-5807) and maintained in RPMI 1640 nutrient mixture with 10% heat-inactivated FBS, 2 mM L-glutamine, 100 units/mL penicillin and 100 μg/mL streptomycin. Cells were incubated at 37 °C in a humidified atmosphere containing 5% CO_2 and were passaged every 3 days at a 1:3 dilution. Cultured cells with passage number 10 to 30 were used in the experiments to reduce variability during cell culture.

B[*a*]P Metabolites in H358 Cell Culture

Induction experiments with TCDD (10 nM) or ethacrynic acid (EA) (70 μM), were performed in 10-mL RPMI/FBS medium for 15 h followed by [^{3}H]-B[*a*]P treatment (4 μM, 2 × 10^6 cpm/nmol, 0.5% DMSO) in 2-mL HBSS. Before harvesting the treated cells, 0.5 nmol of B[*a*]P-4,5-diol was added to cell culture dishes as an internal standard to normalize for losses in the sample work-up and analysis. The total cell culture mixture was harvested by a cell scraper into a 10-mL tube and extracted twice with 3-mL water-saturated ethyl acetate. After centrifugation at 2500 × *g* for 10 min the organic and aqueous extracts were analyzed by scintillation counting to determine the metabolite distribution in the two phases. The organic extract was dried under *vacuo*. The residue was re-dissolved in 150-μL methanol and a 60-μL aliquot was subjected to chromatographic analysis. Quantitation of B[*a*]P metabolites generated in the cells was accomplished using a tandem Waters Alliance 2695 chromatographic system (Waters Corp., Milford, MA) with a Waters 996 photodiode array (PDA) detector and a β-RAM in-line radioactive detector (IN/US Systems Inc., Tampa, FL) as previously published (47). Chromatography was conducted on a reversed-phased (RP) column (Zorbax-ODS C18, 5 μm, 4.6 mm × 250 mm, DuPont Co., Wilmington, DE) at a flow-rate of 0.5 mL/min using the following linear gradient: MeOH/H_2O (v/v) 55-70% (20 min), 70-80% (10 min), 80% (20 min), 80-95% (10 min), and 95% (20 min). Eluates from the column were introduced into the online radiometric detector following mixture of the scintillant with the HPLC effluent (IN/US system Inc.) at a flow rate 1.5 mL/min. The IN/US detector was calibrated by injecting know amounts of B[*a*]P determined by scintillation counting directly into the detector to determine counting efficiency (59.5%). The counting efficiency of the detector was unaffected by the composition of the mobile-phase. The detector was then programmed to correct the output signal to a cpm value. A macro was written to covert corrected cpm to dpm, which were then converted to nmoles using the specific radioactivity of the isotope.

Identification of B[*a*]P Metabolites in Human Bronchoalveolar H358 Cells by LC-MS

The cells (~ 2 × 10^7) were treated with non-radiolabelled B[*a*]P (final 4 μM, 0.5% DMSO) in 2-mL HBSS for 12 h. The culture mixtures were extracted with two vols of ethyl acetate and the organic extract was dried under *vacuo*. The residue was re-dissolved with 50 μL methanol and an 80-μL aliquot of the pooled solution was subjected to LC-MS analysis. Mass spectrometric data were acquired using a Finnigan TSQ Quantum Ultra spectrometer (Thermo Fisher, San Jose, CA) equipped with an atmospheric pressure chemical ionization (APCI)

source. The mass spectrometer was operated in the positive ion mode. On-line chromatography was performed using a Waters Alliance 2690 HPLC system (Waters Corp., Milford, MA). A RP column (Zorbax-ODS C18, 5 μm, 4.6 mm × 250 mm, DuPont Co., Wilmington, DE) was used at a flow-rate of 0.5 mL/min. Solvent A was 5 mM ammonium acetate in water containing 0.02% formic acid, and solvent B was 5 mM ammonium acetate in methanol containing 0.02% formic acid. Chromatography was conducted using the following linear gradient: 55% to 70% methanol (v/v) over 20 min, 70% to 80% methanol (v/v) for 10 min, 80% methanol (v/v) for 20 min, and 80% to 95% methanol (v/v) for 10 min. The eluant on-line was monitored by the mass spectrometer using selected reaction monitoring (SRM) and Q3 full scan modes. The mass spectrometry parameters including discharge current (30 μA), vaporization temperature (470 °C), Sheath Gas (0.525 L/min), ion sweep gas (0.3 L/min), Auxiliary gas (1.5 L/min), capillary temperature (190 °C), tube lens offset (232 V), source CID (-5 V), scan time (0.5 sec) and scan width (0.5 m/z) were automatically optimized with authentic standard compound solutions. SRM transitions for the metabolites were *m/z* 269 → *m/z* 251 for B[*a*]P-dihydrodiols (7,8- and 9,10-dihydrodiol), *m/z* 269 → *m/z* 251 for 3-OH-B[*a*]P, *m/z* 303 → *m/z* 285 for B[*a*]P-tetraol-1, *m/z* 283 → *m/z* 255 for B[*a*]P-quinones (7,8-, 1,6-, and 3,6-dione), and *m/z* 253 for B[*a*]P. The corresponding mass spectrum of each metabolite was obtained from Q3 Full Scan. Identification of the metabolite peaks was achieved by comparing chromatographic retention time and mass spectra of the metabolites with those obtained for the authentic synthetic standards.

Analysis of Aqueous Metabolites

Aliquots of the remaining aqueous phase were processed in four steps. First, the media was neutralized and extracted with ethyl-acetate. Second, the media was neutralized and treated with β-glucuronidase 50 units/mL (*E. coli* Type VIII, Sigma) and the released metabolites extracted with ethyl actetate. Third, the media was adjusted to pH 5.0 and extracted with ethyl acetate, and fourth the media was adjusted to pH 5.0, treated with aryl sulfatase 5 units/mL (*Abalone entrails*, Type VIII β-glucuronidase free Sigma) and the released metabolites extracted with ethyl acetate. No radioactivity was released by these methods. The aqueous metabolites were also analyzed by ion-pair RP-HPLC using a linear gradient of 2 - 60% acetonitrile containing 0.1% acetic acid.

RNA Isolation and Northern Analysis

Cellular RNA was isolated from 2×10^7 cells using Trizol reagent following either treatment with either 4 μM B[*a*]P for 0, 1, 2, 3, 6, 12, 24 h or treatment with 70 μM EA for 15 h in HBSS. Total RNA (30 μg) was separated by electrophoresis on 1% agarose/formaldehyde gels and transferred overnight to the Hybond-N^+ nylon membrane (Amersham Biosciences UK Ltd., Little Chalfont, Bucks). The membrane was hybridized to a cDNA probe containing a fragment of the open reading frame of either AKR1C1 (GenBank accession number: NM_001353, +251 to +972 bp) or human P4501B1 (GenBank accession number: NM_000104, +385 to +1584 bp). Random priming was conducted with radiolabeled [^{32}P]-α-dCTP, and a final specific activity greater than 10^9 cpm/μg of DNA fragment was obtained. Hybridization was performed in ExpressHyb hybridization solution (ClonTech, Palo Alto, CA) at 65 °C for 1 h, and the blot was subjected to a wash with 2 × SSC/0.1% SDS for 10 min at room temperature, and a wash with 0.2 × SSC/0.1% SDS for 10 min at 60 °C. The blot was then exposed to X-ray film at -80 °C overnight. To confirm equally loading of each RNA sample, 28S and 18S rRNA on agarose/formaldehyde gels were visualized by ethidium bromide under a UV transilluminator at 300 nm and photographed.

Results

B[*a*]P Metabolites in Human Bronchoalveolar H358 Cells

To identify B[*a*]P metabolites generated in H358 cells we first exposed parental naïve cells to 4 μM B[*a*]P. Two analytical methods were utilized RP-HPLC-with in line PDA and radiometric detection, or LC-atmospheric chemical ionization (APCI)/MS. The first method, which utilized [^{3}H]-B[*a*]P provided an assessment of the complete metabolic profile and mass balance and permitted the detection of both known and unknown metabolites. The second method utilized unlabeled B[*a*]P and provided rigorous structural identity of the known metabolites. In the two methods the major B[*a*]P metabolites were assigned according to the retention time of the chromatographic peaks and/or by comparison of mass spectra to those obtained with the corresponding authentic synthetic standards. Eight significant metabolite peaks in the radio-chromatogram (Figure 2A,B) were assigned as B[*a*]P-tetraol-1 (M1, tr = 15.9 min), B[*a*]P-9,10-dihydrodiol (M2, tr = 20.7 min), B[*a*]P-7,8-dihydrodiol (M3, tr = 35.0 min), B[*a*]P-7,8-dione (M4, tr = 40.4 min), B[*a*]P-1,6-dione (M5, tr = 45.1 min), B[*a*]P-3,6-dione (M6, tr = 47.1 min), 3-OH-B[*a*]P (M7, tr = 59.2 min), and B[*a*]P (M8, tr = 78.0 min) based on their LC-UV-chromatogram (348 nm) (Figure 2A, B) and co-elution with authentic standard compounds. The metabolite, which eluted at tr = 5.9 min was not identified and was regarded as a polar phase II conjugate due to its poor retention on the column.

Relative quantities of the metabolites were determined using the specific radioactivity of the [^{3}H]-B[*a*]P starting material, Figure 3A. 3-OH-B[*a*]P and B[*a*]P-dihydrodiols were the most prominent primary metabolites followed by the secondary metabolites: B[*a*]P-tetraol-1, B[*a*]P-7,8-dione and B[*a*]P-1,6-/3,6-diones. Over 80% of B[*a*]P was consumed during a 24 h incubation, Figure 3B. Radioactivity in organic extracts markedly decreased to about 40% of the total and a concomitant increase in radioactivity in the aqueous phase was noted, suggesting that B[*a*]P was metabolically converted to water-soluble metabolites. Attempts were made to identify the aqueous soluble metabolites by treatment with either β-glucruonidase or aryl sulfatase but these treatments failed to release radioactivity for extraction. Ion-pair RP-HPLC of the aqueous phase showed at least six minor radioactive peaks. LC/MS/MS in selected ion scan and precursor ion scan modes failed to detect transitions that could be assigned to either a glucuronide or sulfate conjugate suggesting that they are either glutathionyl or mercapturic acid conjugates. At the end of the incubation 20% of radioactivity was retained in the cells and may be present as macromolecule adducts, Figure 3C.

Replicate experiments were then performed with unlabeled B[*a*]P and the M1 to M8 metabolites were identified using LC-MS by comparison with SRM chromatograms (Figure 4A and 4B) and mass spectra (see, Figure 4C and Supplemental Material, Figure S-1) obtained form authentic standards. B[*a*]P-tetraol-1 and B[*a*]P-dihydrodiols (B[*a*]P-7,8-dihydrodiol and B[*a*]P-9,10-dihydrodiol) formed $[M+H-H_2O]^+$ parent ions and product ions $[M+H-2H_2O]^+$ which showed an additional loss of a H_2O molecule. 3-OH-B[*a*]P generated the $[M+H]^+$ parent ion which lost a molecule of water when subjected to collision induced dissociation (CID). B[*a*]P-diones (B[*a*]P-7,8-, 1,6-, and 3,6-dione) formed $[M+H]^+$ parent ions and $[M+H-CO]^+$ product ions when subjected to CID. B[*a*]P generated $[M+H]^+$ that did not fragment. Therefore, eight metabolites were detected under the following SRM transitions: *m/z* 303 $[M+H-H_2O]^+$ → *m/z* 285 $[M+H-2H_2O]^+$ for B[*a*]P-tetraol-1; *m/z* 269 $[M+H-H_2O]^+$ → *m/z* 251 $[M+H-2H_2O]^+$ for B[*a*]P-dihydrodiols (B[*a*]P-7,8- and 9,10-dihydrodiol); *m/z* 283 $[M+H]^+$ → *m/z* 255 $[M+H-CO]^+$ for B[*a*]P-quinones (B[*a*]P-7,8-, 1,6-, and 3,6-dione); *m/z* 269 $[M+H]^+$ → *m/z* 251 $[M+H-H_2O]^+$ for 3-OH-B[*a*]P; and *m/z* 253 $[M+H]^+$ for B[*a*]P.

Induction of P4501B1 and AKR1C1 by B[*a*]P in H358 cells

To verify that H358 cells have inducible P4501B1 and AKR1C1, Northern blotting analysis was performed to detect induction of P4501B1 and/or AKR1C1 by TCDD (an AhR agonist), by B[*a*]P (a bifunctional inducer) and by EA (a monofunctional inducer).

The results showed that P4501A1/1B1, AKR1A1 and AKR1C1 were not constitutively expressed in parental cells, however, P4501B1 and AKR1C1 were significantly upregulated by TCDD (10 nM, 15 h) and EA (70 μM, 15 h), respectively, (see Supplemental Material, Figure S-2). B[*a*]P induced both P4501B1 and AKR1C1 expression in a time-dependent manner, suggesting that chronic exposure to B[*a*]P stimulates its own metabolism through both the diol-epoxide and o-quinone pathways, Figure 5. A lag-phase was observed between the induction of P4501B1 and the induction of AKR1C1 by B[*a*]P and is consistent with the need to metabolize B[*a*]P to an electrophilic metabolite that will then activate the Keap-1/Nrf2 pathway to stimulate the ARE in the AKR1C gene promoter (18). The AKR1C cDNA probe utilized cannot distinguish between AKR1C1-AKR1C3 since they share greater than 86% sequence identity. However, the AKR1C isoform most induced by an ARE in HepG2 cells is AKR1C1 (18).

The P4501B1-Inducer TCDD Eliminates the Lag-phase of B[*a*]P Metabolite Formation

Ideally we would prefer to measure B[*a*]P-metabolism following chronic exposure to this PAH to induce the metabolic pathways. However, we were concerned that residual B[*a*]P would compromise the metabolic profiles and LC-MS analysis. Therefore we elected to measure B [*a*]P-metabolism in the cells following prior exposure to TCDD, Figure 6.

In un-induced cells, B[*a*]P-metabolism was characterized by the formation of 3-OH-B[*a*]P, B [*a*]P-7,8-dihydrodiol, B[*a*]P-tetraol-1 and B[*a*]P-7,8-dione, that reached a maximum after 12 h. The appearance of each of these metabolites was accompanied by a significant lag-phase consistent with enzyme induction. The one exception was B[*a*]P-3,6-dione, whose formation was immediate. Importantly, the formation of B[*a*]P-7,8-dihydrodiol preceded the formation of B[*a*]P-tetraol-1 and B[*a*]P-7,8-dione providing evidence for a precursor-product relationship. After the 12 h time point there was a significant decline in B[*a*]P-7,8-dihydrodiol, whereas the levels of the B[*a*]P-tetraol-1 and B[*a*]P-7,8-dione peaks remained unaltered. This suggests that B[*a*]P-7,8-diol was likely conjugated by phase II enzymes. Induction by TCDD led to the elimination of the lag-phases observed for the formation of B[*a*]P-7,8-dihydrodiol, 3-OH-B[*a*]P, B[*a*]P-tetraol-1 and B[*a*]P-7,8-dione. The exception was B[*a*]P-3,6-dione since no lag-phase was seen in its formation to begin with. Time courses in the TCDD treated cells showed that the formation of B[*a*]P-7,8-dihydrodiol still preceded the formation of B[*a*]P-tetraol-1 and B[*a*]P-7,8-dione demonstrating that the precursor-product relationship was retained. Interestingly, induction with TCDD did not result in elevated levels of B[*a*]P-tetraol-1, B[*a*]P-7,8-dione or 3-OH-B[*a*]P; the appearance of the metabolites just occurred at a faster rate.

Discussion

PAH are a major class of chemical carcinogen found in tobacco smoke and fine particulate matter; and thus human lung epithelial cells are a major site of inhalation exposure. However, little information exists concerning the metabolic activation and fate of PAH in human lung cells. In this study, we used parental H358 cells (transformed bronchoalveolar cells of epithelial orgin) to study B[*a*]P-metabolism by RP-HPLC with in line photo-diode array and radiometric detection and by LC/APCI/MS. Three pathways of metabolic activation have been proposed to exist, the peroxidase pathway (which forms radical cations), the P4501A1/1B1 plus EH pathway (which forms diol-epoxides), and the P501A1/1B1, EH plus AKR pathway (which

forms *o*-quinones). Each pathway can give rise to distinctive metabolites, e.g. B[*a*]P-1,6-dione and B[*a*]P-3,6-dione (peroxidase), B[*a*]P-tetraols (P4501A1/1B1 plus EH) and B[*a*]P-7,8-dione (P4501A1/1B1, EH plus AKR). Evidence for the formation of all three metabolites were obtained, suggesting that each metabolic pathway exists in human lung cells and may contribute to lung carcinogenesis. The formation of B[*a*]P-1,6-dione and B[*a*]P-7,8-dione suggest that the lung can produce two different redox-active metabolites capable of producing ROS, and ROS-derived oxidative DNA damage (that can potentially result in mutations) upon PAH exposure.

Induction with TCDD and its effects on metabolic profiles was revealing. In the absence and presence of TCDD a precursor-product relationship existed between B[*a*]P-7,8-dihydrodiol and the appearance of B[*a*]P-tetraol-1 and B[*a*]P-7,8-dione suggesting that the diol was the precursor of both these metabolites. Importantly, the levels of B[*a*]P-tetraol-1 and B[*a*]P-7,8-dione formed were unaltered by TCDD induction, instead their formation just occurred earlier. This suggests that TCDD (P450 inducer) and B[*a*]P (a P450 and AKR1C1 inducer) ultimately yield the same B[*a*]P-metabolic profile. B[*a*]P is a bifunctional inducer that works through the XRE and ARE, whereas TCDD works only through the XRE (18). However, exposure of TCDD induced cells to B[*a*]P will likely produce the requisite electrophilic metabolite responsible for AKR induction, and hence the metabolic profiles are ultimately similar.

A surprise in the induction experiments were the data obtained for the radical-cation metabolite B[*a*]P-3,6-dione. This metabolite formed immediately in the absence or presence of TCDD and suggests that the B[*a*]P-3,6-dione is not derived from 3-OH-B[*a*]P since the formation of this latter metabolite required enzyme induction. These data also suggest that the peroxidase required for B[*a*]P-3,6-dione formation is neither P4501A1 nor P4501B1 since these P450 isoforms required induction. Thus the peroxidase responsible for the formation of B[*a*]P-3,6-dione remains unidentified. Previously, incubation of B[*a*]P with arachidonic acid and ram seminal vesicles resulted in the formation B[*a*]P-1,,6-, 3,6-, and 6,12-diones on the same time course as prostaglandin (PG)H_2 production suggesting that B[*a*]P acts as a co-reductant in the peroxidase cycle of PGH synthase (53). Other peroxidases implicated in the formation of these diones are lactoperoxidase (an airway peroxidase) (54).

Two of the organic soluble metabolites, B[*a*]P-7,8-dihydrodiol and 3-OH-B[*a*]P showed a dramatic decline in levels after reaching a peak suggesting that they were forming water soluble conjugates. The presence of water soluble conjugates is notable in the mass balance since up to 40% of B[*a*]P becomes aqueous soluble. Treatment of the aqueous phase with either β-glucuronidase or sulfatase failed to liberate radioactivity that was organic extractable suggesting the presence of other water-soluble conjugates e.g. GSH or mercapturic acid metabolites

Knowledge of the metabolic profiles described in the present study has two major utilities. First, they can identify the major routes of PAH activation in lung and second they can be used to identify the most valuable biomarkers for PAH inhalation exposure in terms of detecting urinary and plasma metabolites. With regard to PAH activation, we have shown that when parental H358 cells are exposed to B[*a*]P the formation of (+)-*trans*-*anti*-B[*a*]PDE-N^2-dGuo adducts occurred without a lag-phase. Moreover, more (+)-*trans*-*anti*-B[*a*]PDE-N^2-dGuo adducts were formed in parental cells treated with (-)-B[*a*]P-7,8-dihydrodiol than in cells treated with TCDD (55). Thus, while diol-epoxides are the source of these adducts, and B[*a*]P-tetraol-1 levels may reflect *anti*-B[*a*]PDE formation, the enzyme system responsible for diol-epoxide-DNA adduct formation may not be P4501A1/1B1. This view was supported by the inability of 2,4,3′,5′-tetramethylstilbene, a P4501A1/1B1 inhibitor, to block *anti*-B[*a*]PDE adduct formation (unpublished data Gelhaus and Blair). Other P450's that are expressed in human lung cells include, 2A6, 2A13, 2B6, 2E1, 2C18, 2F1, 2J2, 2S1, 3A5 and 4B1 (56-60).

Of these, P450 3A5 has been shown to catalyze the metabolism of (-)-B[*a*]P-7,8-dihydrodiol to form (+)-*anti*-B[*a*]PDE (61). The rapid formation of *anti*-B[*a*]PDE in the TCDD treated cells may instead lead to improved detoxication rather than DNA-adduct formation. We have suggested that induction of P4501A1/1B1 may provide a protective mechanism against *anti*-B[*a*]PDE-N^2-dGuo adduct formation (55).

The most widespread biomarker of PAH exposure has been 1-hydroxypyrene, since pyrene is present in many PAH mixtures (62,63). However, pyrene is not carcinogenic by itself. Since B[*a*]P is now considered by IARC as a human carcinogen it would be superior to have a biomarker of response based on its exposure (64). The abundance of 3-OH-B[*a*]P in our studies suggest that this metabolite may be a superior biomarker of exposure to carcinogenic PAH than 1-hydroxypyrene. Several studies have been performed to validate this metabolite as a biomarker. The largest single problem has been one of sensitivity, since levels of 3-OH-B[*a*]P are 10^3 to 10^5 less than that seen for 1-hydroxypyrene (63). Attempts to solve this problem have utilized LC-APCI/MS methodology with some success (62). The remaining issue is that 3-OH-B[*a*]P does not reflect levels of B[*a*]P metabolites that would have carcinogenic properties. By contrast, the formation of metabolites that come from electrophiles that are able to form lesions with DNA, e.g. B[*a*]P-tetraol-1 (*anti*-B[*a*]PDE), B[*a*]P-3,6-dione (radical cation) and B[*a*]P-7,8-dione (*o*-quinone) suggest that levels of these metabolites might be used as superior biomarkers of PAH exposure and response. Progress in detecting and quantitating B[a]P-tetraol-1 in human urine by GC/negative-ion (NI)CI/MS has been reported (65). This method gave fmol sensitivity and could detect B[*a*]P exposures in psorarsis patients receiving coal-tar treatments, steel workers, an smokers. Lowest levels were observed in smokers, and in some smokers B[*a*]P-tetraol-1 was not detected suggesting that increased sensitivity may be desirable.

In summary, we have conducted studies on the metabolism of B[*a*]P in human lung cells using LC/APCI/MS methodologies. We provide evidence for the existence of three pathways of B[*a*]P activation which include the formation of radical cations, diol-epoxides, and *o*-quinones. Measurement of the respective organic soluble metabolites from each of these pathways suggest that they are relatively minor with respect to the formation of 3-hydroxy-B[*a*]P. The contributions of each of these pathways to B[*a*]P-activation based on the relative abundance of their respective DNA-adducts in lung cells remains to be addressed.

Acknowledgements

This work was supported by grants R01 CA39504 and P01 CA92537 awarded to T.M.P. and by P30 ES013508-01. The contents of this publication are solely the responsibility of the authors and do not necessarily represent the official views of NIEHS and NIH.

Abbreviations

AhR, aryl hydrocarbon receptor
AKR, aldo-keto reductase
APCI, atmospheric pressure chemical ionization
ARE, anti-oxidant response element
t-BHQ, *tert*-butylhydroquinone
B[*a*]P, benzo[*a*]pyrene
anti-B[*a*]PDE, *anti*-B[*a*]P-7,8-diol-9,10-epoxide
dGuo, deoxyguanosine
dAdo, deoxyadenosine
B[*a*]P -7,8-dihydrodiol, (±)-*trans*-7,8-dihydroxy-7,8-dihydro-benzo[*a*]pyrene
B[*a*]P -9,10-dihydrodiol, (±)-9,10-*trans*-dihydroxy-9,10-dihydro-benzo[*a*]pyrene
B[*a*]P-1,6-dione, benzo[*a*]pyrene-1,6-dione

B[*a*]P-3,6-dione, benzo[*a*]pyrene-3,6-dione
B[*a*]P-6,12-dione, benzo[*a*]pyrene-6,12-dione
B[*a*]P-7,8-dione, benzo[*a*]pyrene-7,8-dione
B[*a*]P-tetrol-1, *r*-7,*t*-8,*t*-9,*c*-10-tetrahydroxy-7,8,9,10-tetrahydrobenzo[*a*]pyrene
EA, ethacrynic acid
EH, epoxide hydrolase
FBS, fetal bovine serum
GST, glutathione-S-transferases
HBSS, Hank's balanced salt solution
LC/APCI/MS, liquid chromatography/atmospheric pressure chemical ionization/mass spectrometry
Nrf2, nuclear factor E2-related factor 2
3-OH- B[*a*]P, 3-hydroxy-B[*a*]P
P450, cytochrome P450
PAH, polycyclic aromatic hydrocarbon
ROS, reactive oxygen species
SDS, sodium dodecyl sulfate
TCDD, 2,3,7,8-tetrachlorodibenzo-*p*-dioxin
XRE, xenobiotic response element

References

(1). Ries, I.; Eisner, MP.; Kosary, CL. SEER Cancer Statistics Review 1975-2006: National Cancer Institute. 2006. http//SEER.cancer.gov/esr

(2). WHO, W.H.O. Tobacco Habits Other than Smoking; Betel-Quid and Areca-Nut Chewing; and Some Related Nitrosamines; ISBN 92 832 1537 0. IARC Monograph 1985;37

(3). WHO, W.H.O.. International Programme on Chemical Safety. Geneva, Switzerland: 1998. Selected non-heterocyclic polycyclic aromatic hydrocarbons IPCS.

(4). Hoffmann, D.; Hecht, SS. Advances in tobacco carcinogenesis. In: Cooper, CS.; Grover, PL., editors. Handbook of experimental pharmacology. Springer-Verlag; Heidelberg (Germany): 1990. p. 63-102.

(5). Hecht SS. Tobacco smoke carcinogens in lung cancer. J. Natl. Cancer Inst 1999;91:1194–1210. [PubMed: 10413421]

(6). IARC. Polynuclear aromatic compounds. Part 1. Chemical, environmental and experimental data. IARC Monograph Evaluation of Carcinogenic Risk Chem Hum 1983;32:1–453.

(7). Scherer G, Frank S, Riedel K, Meger-Kossien I, Renner T. Biomonitoring of exposure to polycyclic aromatic hydrocarbons of nonoccupationally exposed persons. Cancer Epidemiol. Biomarkers Prev 2000;9:373–380.

(8). Vyskocil A, Fiala Z, Fialova D, Krajak V, Viau C. Environmental exposure to polycyclic aromatic hydrocarbons in Czech Republic. Hum. Exp. Toxicol 1997;16:589–595. [PubMed: 9363476]

(9). Cavalieri E, Rogan EG. Central role of radical cations in the metabolic activation of polycyclic aromatic hydrocarbons. Xenobiotica 1995;25:677–688. [PubMed: 7483666]

(10). Devanesan PD, RamaKrishna NVS, Todorovic R, Rogan EG, Cavalieri EL, Jeong H, Jankowiak R, Small GJ. Identification and quantitation of benzo[*a*]pyrene-DNA adducts formed by rat liver microsomes in vitro. Chem. Res. Toxicol 1992;5:302–309. [PubMed: 1643262]

(11). Devanesan PD, Higginbotham S, Ariese F, Jankowiak R, Suh M, Small GJ, Cavalieri E, Rogan E. Depurinating and stable benzo[*a*]pyrene-DNA adducts formed in isolated rat liver nuclei. Chem. Res. Toxicol 1996;9:1113–1116. [PubMed: 8902265]

(12). Cavalieri, E.; Rogan, EG. Fluoro-substitution of carcinogenic aromatic hydrocarbons: models for understanding mechanisms of metabolic activation and oxygen transfer catalyzed by cytochrome P450. In: Neilson, AH., editor. The Handbook of Environmental Chemistry. 3. Part N Organofluorines. Springler-Verlag; Berlin-Heidelberg: 2002.

(13). Lorentzen RJ, Caspary WJ, Lesko SA, Ts'o POP. The autoxidation of 6-hydroxybenzo[*a*]pyrene and 6-oxobenzo[*a*]pyrene radical, reactive metabolites of benzo[*a*]pyrene. Biochemistry 1975;14:3970–3977.

(14). Flowers-Geary L, Harvey RG, Penning TM. Examination of polycyclic aromatic hydrocarbon *o*-quinones produced by dihydrodiol dehydrogenase as substrates for redox-cycling in rat liver. Biochem. (Life. Sci.Adv) 1992;11:49–58.

(15). Lorentzen RJ, Ts'o POP. Benzo[*a*]pyrenedione/benzo[*a*]pyrenediol oxidation-reduction couples and the generation of reactive reduced molecular oxygen. Biochemistry 1977;16:1467–1473. [PubMed: 191070]

(16). Gelboin HV. Benzo[*a*]pyrene metabolism, activation and carcinogenesis: Role and regulation of mixed function oxidases and related enzymes. Physiol. Rev 1980;60:1107–1166. [PubMed: 7001511]

(17). Conney AH. Induction of microsomal enzymes by foreign chemicals and carcinogenesis by polycyclic aromatic hydrocarbons. G.H.A. Clowes Memorial Lecture. Cancer Res 1982;42:4875–4917. [PubMed: 6814745]

(18). Burczynski ME, Lin H-K, Penning TM. Isoform-specific induction of a human aldo-keto reductase by polycyclic aromatic hydrocarbons (PAHs), electrophiles, and oxidative stress: implications for the alternative pathway of PAH activation catalyzed by human dihydrodiol dehydrogenases. Cancer Res 1999;59:607–614. [PubMed: 9973208]

(19). Penning TM, Burczynski ME, Hung C-F, McCoull K, Palackal N, Tsuruda LS. Dihydrodiol dehydrogenases and polycyclic aromatic hydrocarbon activation: Generation of reactive and redox active *o*-quinones. Chem. Res. Toxicol 1999;12:1–18. [PubMed: 9894013]

(20). Palackal NT, Burczynski ME, Harvey RG, Penning TM. The ubiquitous aldehyde reductase (AKR1A1) oxidizes proximate carcinogen *trans*-dihydrodiols to *o*-quinones: Potential role in polycyclic aromatic hydrocarbon activation. Biochemistry 2001;40:10901–10910. [PubMed: 11535067]

(21). Palackal NT, Lee SH, Harvey RG, Blair IA, Penning TM. Activation of polycyclic aromatic hydrocarbon *trans*-dihydrodiol proximate carcinogens by human aldo-keto reductase (AKR1C) enzymes and their functional overexpression in human lung carcinoma (A549) cells. J. Biol. Chem 2002;277:24799–24808. [PubMed: 11978787]

(22). Penning TM, Ohnishi ST, Ohnishi T, Harvey RG. Generation of reactive oxygen species during the enzymatic oxidation of polycyclic aromatic hydrocarbon *trans*-dihydrodiols catalyzed by dihydrodiol dehydrogenase. Chem. Res. Toxicol 1996;9:84–92. [PubMed: 8924621]

(23). Flowers-Geary L, Bleczinksi W, Harvey RG, Penning TM. Cytotoxicity and mutagenicity of polycyclic aromatic hydrocarbon *o*-quinones produced by dihydrodiol dehydrogenase. Chem. Biol. Interact 1996;99:55–72. [PubMed: 8620579]

(24). Burdick AD, Davis JW, Liu KJ, Hudson LG, Shi H, Monske ML, Burchiel SW. Benzo[*a*]pyrene quinones increase cell proliferation, generate reactive oxygen species. and transactivate the epidermal growth factor receptor in breast epithelial cells. Cancer Res 2003;63:7825–7833. [PubMed: 14633709]

(25). Malaveille C, Kuroki T, Sims P, Grover PL, Bartsch H. Mutagenicity of isomeric diol-epoxides of benzo[*a*]pyrene and benz[*a*]anthracene in *S. typhimurium* TA98 and TA100 and in V79 chinese hamster cells. Mutat. Res 1977;44:313–326. [PubMed: 333280]

(26). Nesnow S, Ross JA, Stoner GD, Mass MJ. Mechanistic linkage between DNA adducts, mutations in oncogenes and tumorigenesis of carcinogenic environmental polycyclic aromatic hydrocarbons in strain A/J mice. Toxicology 1995;105:403–413. [PubMed: 8571376]

(27). Jennette KW, Jeffery AM, Blobstein SH, Beland FA, Harvey RG, Weinstein IB. Nucleoside adducts from the *in vitro* reaction of benzo[*a*]pyrene-7,8-dihydrodiol-9,10-oxide or benzo[*a*]pyrene-4,5-oxide with nucleic acids. Biochemistry 1977;16:932–938. [PubMed: 843522]

(28). Koreeda M, Moore PD, Wislocki PG, Levin W, Conney AH, Yagi H, Jerina DM. Binding of benzo [*a*]pyrene-7,8-diol-9,10-epoxides to DNA, RNA and protein of mouse skin occurs with high stereoselectivity. Science 1978;199:778–781. [PubMed: 622566]

(29). Marshall CJ, Vousden KH, Phillips DH. Activation of c-Ha-ras-1 proto-oncogene by *in vitro* chemical modification with a chemical carcinogen, benzo[*a*]pyrene diol-epoxide. Nature 1984;310:585–589.

(30). Denissenko MF, Pao A, Tang M-S, Pfieifer GP. Preferential formation of benzo[*a*]pyrene adducts at lung cancer mutational hotspots in p53. Science 1996;274:430–432. [PubMed: 8832894]

(31). Shou M, Harvey RG, Penning TM. Reactivity of benzo[*a*]pyrene-7,8-dione with DNA. Evidence for the formation of deoxyguanosine adducts. Carcinogenesis 1993;14:475–482. [PubMed: 8384091]

(32). Balu N, Padgett WT, Lambert GR, Swank AE, Richard AM, Nesnow S. Identification and characterization of novel stable deoxyguanosine and deoxyadenosine adducts of benzo[*a*] pyrene-7,8-quinone from reactions at physiological pH. Chem. Res. Toxicol 2004;17:827–838. [PubMed: 15206904]

(33). Balu N, Padgett WT, Nelson GB, Lambert GR, Ross JA, Nesnow S. Benzo[*a*]pyrene-7,8-quinone-3′-mononucleotide adduct standards for [^{32}P]- post-labeling analyses: detection of benzo [*a*]pyrene-7,8-quinone-calf thymus DNA adducts. Anal. Biochem 2006;355:213–223. [PubMed: 16797471]

(34). McCoull KD, Rindgen D, Blair IA, Penning TM. Synthesis and characterization of polycyclic aromatic hydrocarbon *o*-quinone depurinating N7-guanine adducts. Chem. Res. Toxicol 1999;12:237–246. [PubMed: 10077486]

(35). Yu D, Berlin JA, Penning TM, Field JM. Reactive oxygen species generated by PAH *o*-quinones cause change-in-function mutations in p53. Chem. Res. Toxicol 2002;15:832–842. [PubMed: 12067251]

(36). Penning TM, Shen YM, Mick R, Shults J, Field JM. Polycyclic aromatic hydrocarbon *o*-quinones mutate p53 in human lung adenocarcinoma (A549) cells. Polycyclic Aromatic Compounds 2004;24:583–596.

(37). Park J-H, Gopishetty S, Szewczuk LM, Troxel AB, Harvey RG, Penning TM. Formation of 8-oxo-7,8-dihydro-2′-deoxyguanosine (8-oxo-dGuo) by PAH *o*-quinones: involvement of reactive oxygen species and copper (II)/copper(I) redox cycling. Chem. Res. Toxicol 2005;18:1026–1037. [PubMed: 15962938]

(38). Shen YM, Troxel AB, Vedantam S, Penning TM, Field JM. Comparison of p53 mutations induced by PAH *o*-quinones with those caused by *anti*-benzo[*a*]pyrene diol epoxide in *vitro*: Role of reactive oxygen and biological selection. Chem. Res. Toxicol 2006;19:1441–1450. [PubMed: 17112231]

(39). Shimada T, Martin MV, Pruess-Schwartz D, Marnett LJ, Guengerich FP. Roles of individual human cytochrome P-450 enzymes in the bioactivation of benzo[*a*]pyrene, 7,8-dihydroxy-7,8-dihydrobenzo[*a*]pyrene and other dihydrodiol derivatives of polycyclic aromatic hydrocarbons. Cancer Res 1989;49:6304–6312. [PubMed: 2509067]

(40). Shimada T, Gillam EMJ, Oda Y, Tsumura F, Sutter TR, Guengerich FP, Inoue K. Metabolism of benzo[*a*]pyrene to *trans*-7,8-dihydroxybenzo[*a*]pyrene by recombinant human cytochrome P4501B1 and purified liver epoxide hydrolase. Chem. Res. Toxicol 1999;12:623–629. [PubMed: 10409402]

(41). Burczynski ME, Harvey RG, Penning TM. Expression and characterization of four recombinant human dihydrodiol dehydrogenase isoforms: Oxidation of *trans*-7,8-dihydroxy-7,8-dihydrobenzo [*a*]pyrene to the activated *o*-quinone metabolite benzo[*a*]pyrene-7,8-dione. Biochemistry 1998;37:6781–6790. [PubMed: 9578563]

(42). Denison MS, Fisher JM, Whitlock JP Jr. The DNA recognition site for the dioxin-Ah receptor complex. Nucleotide sequence and functional analysis. J. Biol. Chem 1988;263:17221–17224. [PubMed: 2846558]

(43). Sutter TR, Tang YM, Hayes CL, Wo Y-Y, Jabs W, Li X, Yin H, Cody CW, Greenlee WF. Complete cDNA sequence of a human dioxin-inducible mRNA identifies a new gene subfamily of cytochrome P450 that maps to chromosome 2. J. Biol. Chem 1994;269:13092–13099. [PubMed: 8175734]

(44). Shimada T, Hayes CL, Yamazaki H, Amin S, Hecht SS, Guengerich FP, Sutter TR. Activation of chemically diverse procarcinogens by human cytochrome P450 1B1. Cancer Res 1996;56:2979–2984. [PubMed: 8674051]

(45). Lou H, Du S, Ji Q, Stolz A. Induction of AKR1C2 by Phase II inducers: Identification of a distal consensus antioxidant response element regulated by Nrf2. Mol. Pharmacol 2006;69:1662–1672. [PubMed: 16478829]

(46). Hsu N-Y, Ho H-C, Chow K-C, Lin T-Y, Shih C-S, Wang L-S, Tsai C-M. Overexpression of dihydrodiol dehydrogenase as a prognostic marker of non-small cell lung cancer. Cancer Res 2001;61:2727–2731. [PubMed: 11289154]

(47). Jiang H, Vudathala DK, Blair IA, Penning TM. Competing roles of aldo-keto reductase 1A1 and cytochrome P4501B1 in benzo[*a*]pyrene-7,8-diol activation in human bronchoalveolar H358 cells: Role of AKRs in P4501B1 induction. Chem. Res. Toxicol 2006;19:68–78. [PubMed: 16411658]

(48). Siegfried JM, Rudo K, Bryant BJ, Ellis S, Mass MJ, Nesnow S. Metabolism of benzo[*a*]pyrene in monolayer cultures of human bronchial epithelial cells from a series of donors. Cancer Res 1986;46:4368–4371. [PubMed: 3731094]

(49). Monteith DK, Novotny A, Michalopouklos G, Strom SC. Metabolism of benzo[*a*]pyrene in primary cultures of human hepatocytes dose-response over a four-log range. Carcinogenesis 1987;8:983–988. [PubMed: 3594730]

(50). Merrick BA, Mansfield BK, Nikbakht PA, Slekirk JK. Benzo[*a*]pyrene metabolism in human T 47D mammary tumor cells: evidence for sulfate conjugation and translocation of reactive metabolites across cell membranes. Cancer Lett 1985;29:139–150. [PubMed: 4075284]

(51). Selkirk JK, Croy RG, Whitlock JP Jr. Gelboin HV. *In vitro* metabolism of benzo[*a*]pyrene by human liver microsomes and lymphocytes. Cancer Res 1975;35:3651–3655. [PubMed: 1192426]

(52). Harvey RG, Dai Q, Ran C, Penning TM. Synthesis of the *o*-quinones and other oxidized metabolites of polycycic aromatic hydrocarbons implicated in carcinogenesis. J. Org. Chem 2004;69:2024–2032. [PubMed: 15058949]

(53). Marnett, LJ. Hydroperoxide-dependent oxygenation of polycyclic aromatic hydrocarbons and their metabolites. In: Harvey, RG., editor. Polycyclic Hydrocarbons and Carcinogenesis, American Chemical Society Symposium Series. 283. 1985. p. 307-326.

(54). Reed M, Monske M, Lauer F, Messerole S, Born J, Burchiel S. Benzo[*a*]pyrene diones are produced by photochemical and enzymatic oxidation and induce concentration-dependent decreases in the proliferative state of human pulmonary epithelial cells. J. Toxicol. Environ. Health 2003;66:1189–205.

(55). Ruan Q, Gelhuas SL, Penning TM, Harvey RG, Blair IA. Aldo-keto reductase and cytochrome P450-dependent formation of benzo[*a*]pyrene-derived DNA adducts in human bronchoalveolar cells. Chem. Res. Toxicol 2007;20:424–431. [PubMed: 17295519]

(56). Shimada T, Yamazaki H, Mimura M, Wakamiya N, Ueng Y-F, Guengerich FP, Inui I. Characterization of microsomal cytochrome P450 enzymes involved in the oxidation of xenobiotic chemicals in human fetal livers and adult lungs. Drug Metab. Dispos 1996;24:515–522. [PubMed: 8723730]

(57). Hukkanen J, Lassila A, Paivarinta K, Vlanne S, Sarpo S, Hakkola J, Pelkonen O, Raunio H. Induction and regulation of xenobiotic-metabolizing cytochrome P450s in the human A549 lung adenocarcinoma cell line. Am. J. Respir. Cell Mol. Biol 2000;22:360–366. [PubMed: 10696073]

(58). Hukkanen J, Pelkonen O, Hakkola J, Raunio H. Expression and regulation of xenobiotic-metabolizing cytochrome P450 (CYP) enzymes in human lung. Crt. Rev. Toxicol 2002;32:391–411.

(59). Castell JV, Donato MT, Gomez-Lechon MJ. Metabolism and bioactivation of toxicants in the lung. The *in vitro* cellular approach. Exp. Toxicol. Pathol 2005;57(Suppl 1):184–204.

(60). Roos PH, Bolt HM. Cytochrome P450 interactions in human cancers: new aspects considering CYP1B1. Expert Opin. Drug Metab. Toxicol 2005;1:187–202. [PubMed: 16922636]

(61). Roberts-Thomson SJ, McManus ME, Tukey RH, Gonzalez FF, Holder GM. The catalytic activity of four expressed human cytochrome P450s towards benzo[*a*]pyrene and the isomers of its proximate carcinogen. Biochem. Biophys. Res. Commun 1993;192:1373–1379. [PubMed: 8507205]

(62). Fan R, Dong Y, Zhang W, Wang Y, Yu Z, Sheng G, Fu J. Fast simultaneous determination of urinary 1-hydroxypyrene and 3-hydroxybenzo[*a*]pyrene by liquid chromatography-tandem mass spectrometry. J. Chromatogr. B 2006;836:92–97.

(63). Lafontaine M, Champmartin C, Simon P, Delsaut P, Funck-Brentano C. 3-Hydroxybenzo[*a*]pyrene in the urine of smokers and smokers. Toxicol. Lett 2006;162:181–185. [PubMed: 16406420]

(64). Straif K, Bann R, Secretan B, El Ghisassi F, Cogliano V. carcinogenicity of polycyclic aromatic hydrocarbons. The Lancet Oncology 2005;6:931–932. [PubMed: 16353404]

(65). Simpson CD, Wu M-T, Christiani DC, Santella RM, Carmella SG, Hecht SS. Determination of r-7,t-8,9,c-10-tetrahydroxy-7,8.9,10-tetrahydro-benzo[*a*]pyrene in human urine by gas chromatography/negative ion chemical ionization/mass spectrometry. Chem. Res. Toxicol 2000;13:271–280. [PubMed: 10775327]

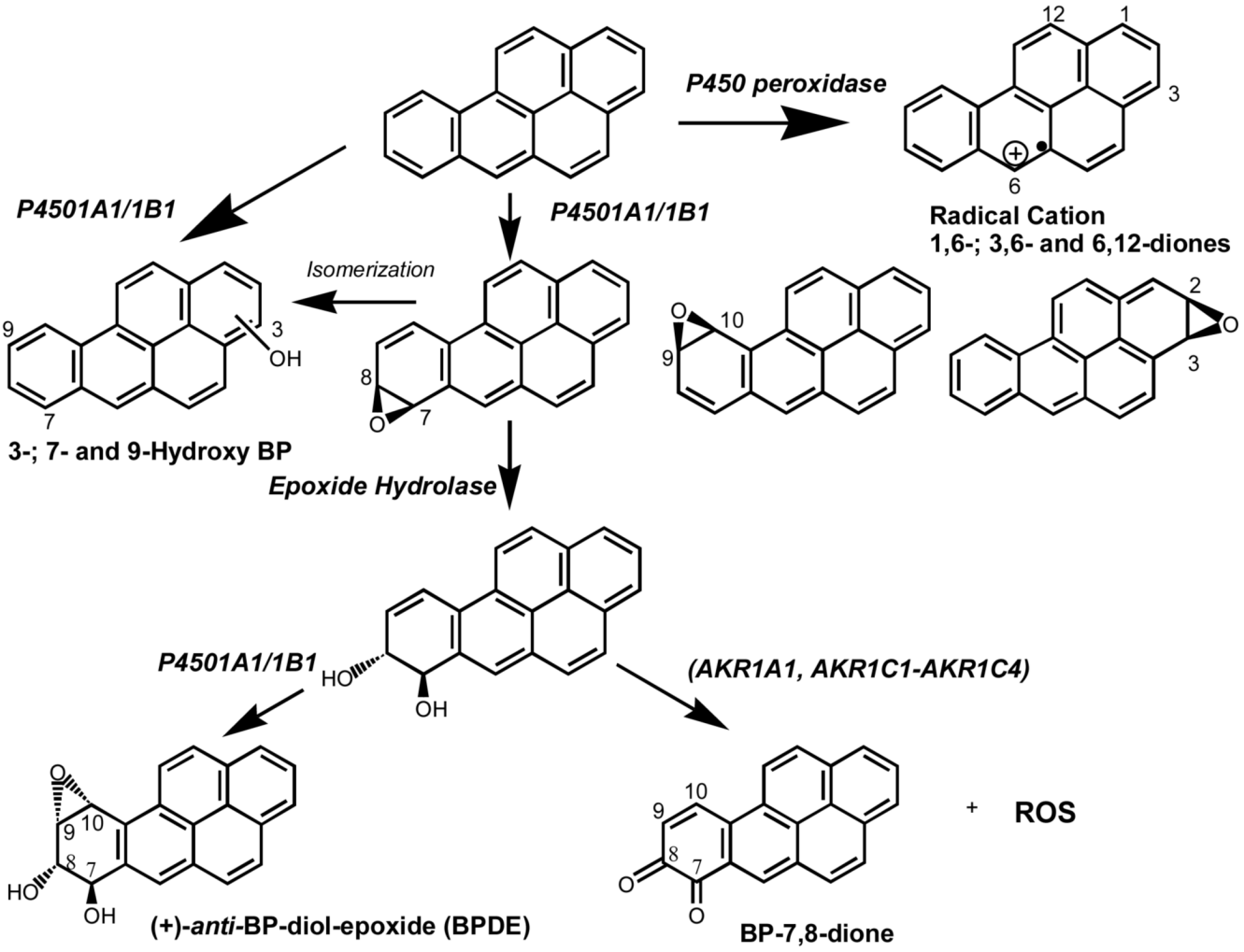

Figure 1.
Metabolic pathways of B[*a*]P in humans.

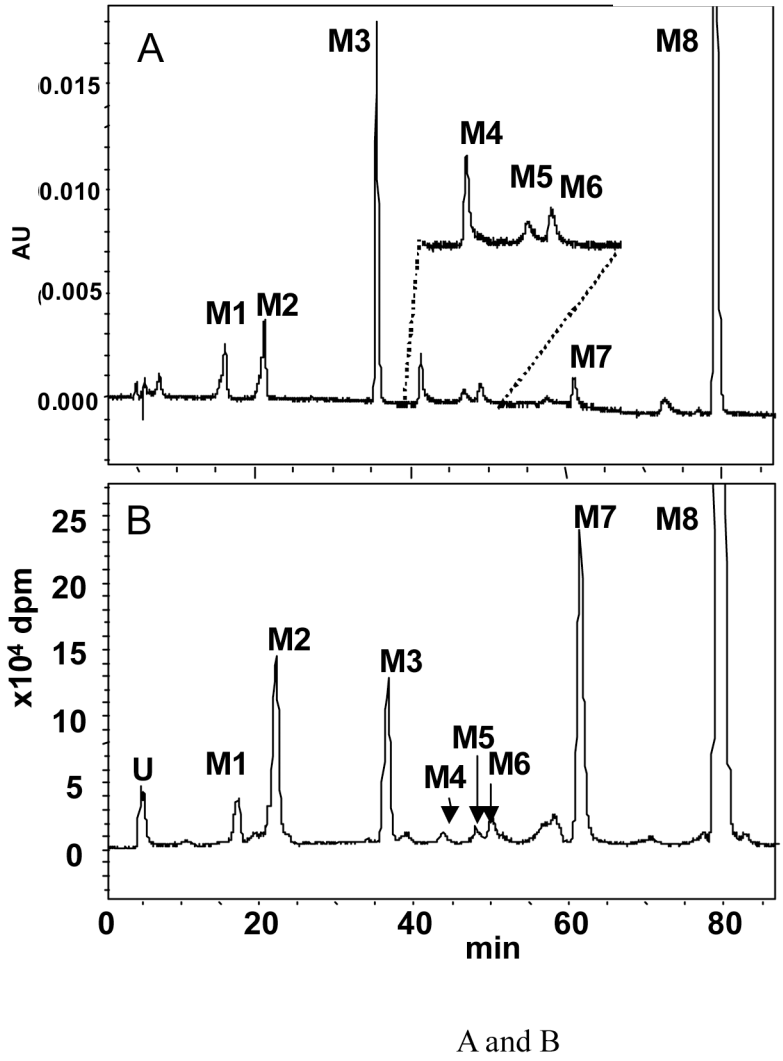

Figure 2.

Chromatographic separation of B[*a*]P-metabolites formed in parental H358 cells: Parental H358 cells (2×10^7) were incubated with 4.0 μM [^{3}H]-B[*a*]P in HBSS plus glucose. Over time aliquots of the culture media were extracted with EtoAC, and the extracts analyzed by reverse phased (RP)-HPLC for B[*a*]P-metabolites by co-elution with authentic standards. Panel A, RP-HPLC chromatograms of the authentic standards acquired with UV detectoion at 348 nm. Peak 1, B[*a*]P-tetrol-1 (M1); peak 2, B[*a*]P-9,10-dihydrodiol (M2); peak 3, B[*a*]P-7,8-dihydrodiol (M3); peak 4, B[*a*]P-7,8-dione (M4); peak 5, B[*a*]P-1,6-dione (M5); peak 6, B[*a*]P-3,6-dione (M6); peak 7, 3-OH-B[*a*]P (M7); peak 8, B[*a*]P (M8); Peak U, unidentified polar metabolite (s). Panel B, radiochromatogram of B[*a*]P-metabolites formed in H358 cells obtained at 12 h.

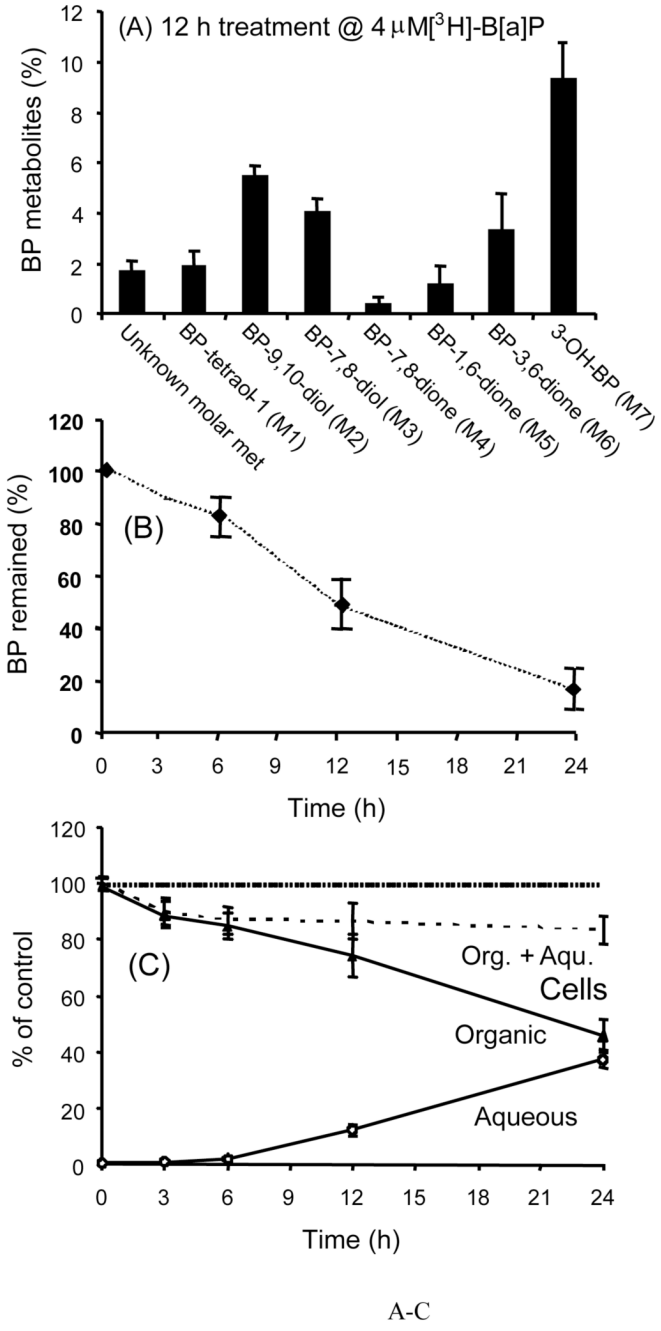

Figure 3.

Quantitation, time-course and mass-balance of B[*a*]P metabolites formed in parental H358 cells. Parental H358 cells (2×10^7) were incubated with 4.0 μM [^{3}H]-B[*a*]P as described in Figure 2. At each time point the amount of B[*a*]P remaining and the total recovery of radioactivity was estimated. The organic and aqueous phases accounted for >85% of the radioactivity at all time points. Panel A, quantitation of individual B[*a*]P metabolites at 12 h. Panel B, time course of [^{3}H]-B[*a*]P consumption, and Panel C, the distribution of radioactivity in the organic and aqueous phases; (○) aqueous metabolites in the culture media; (●) organic metabolites in cell culture medium; and combined aqueous and organic metabolites in the cell lysates (------).

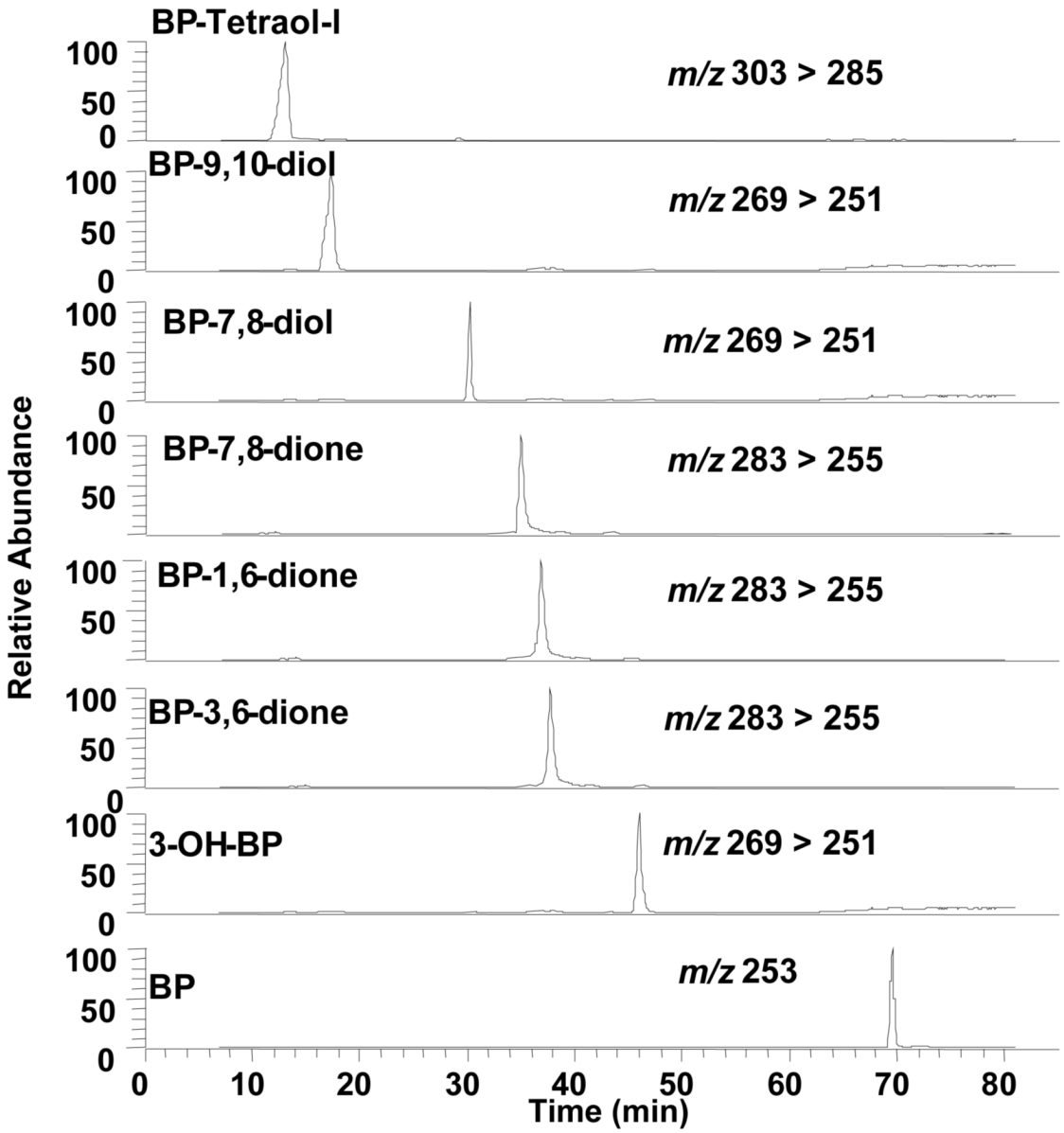

A

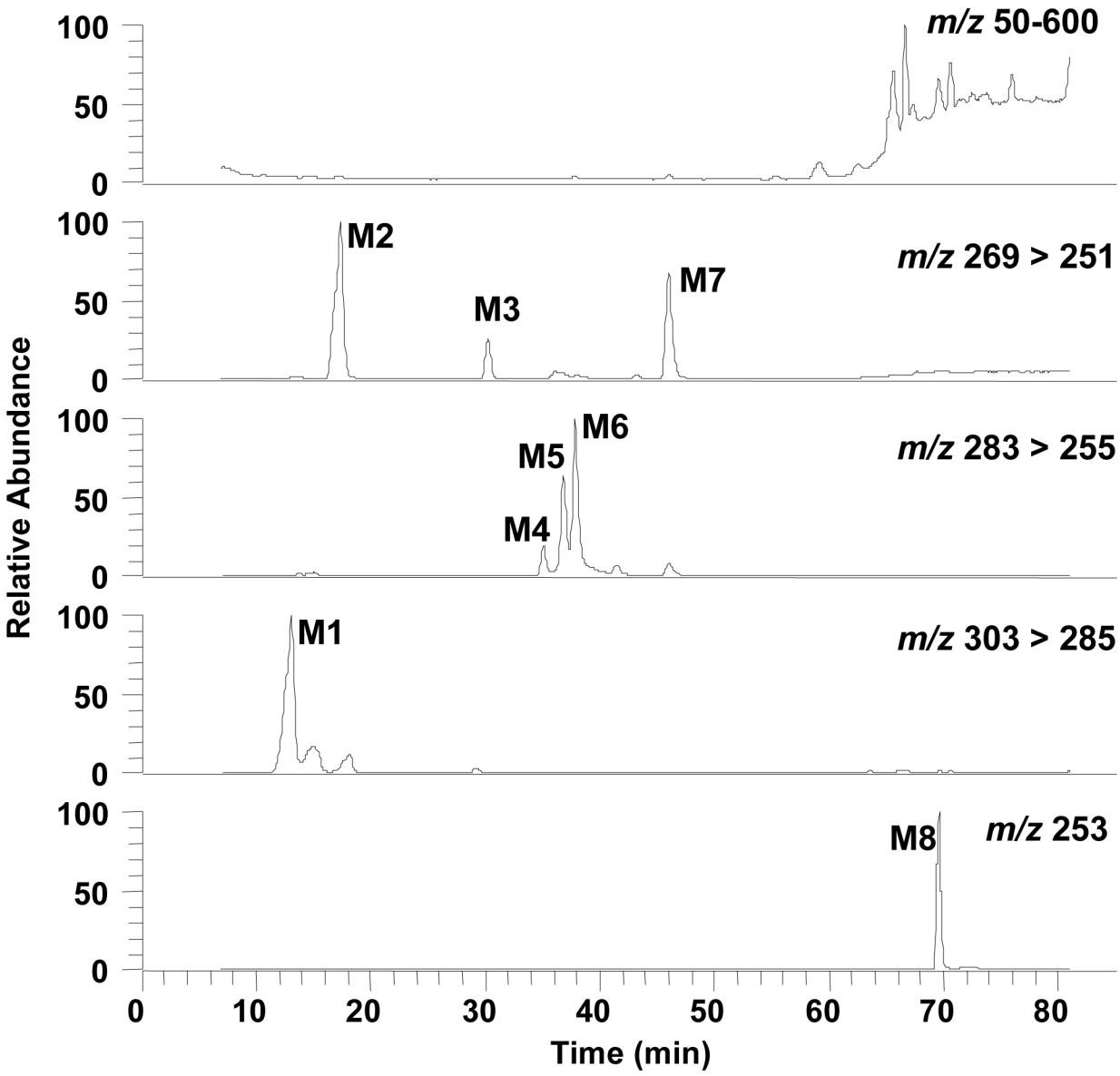

B

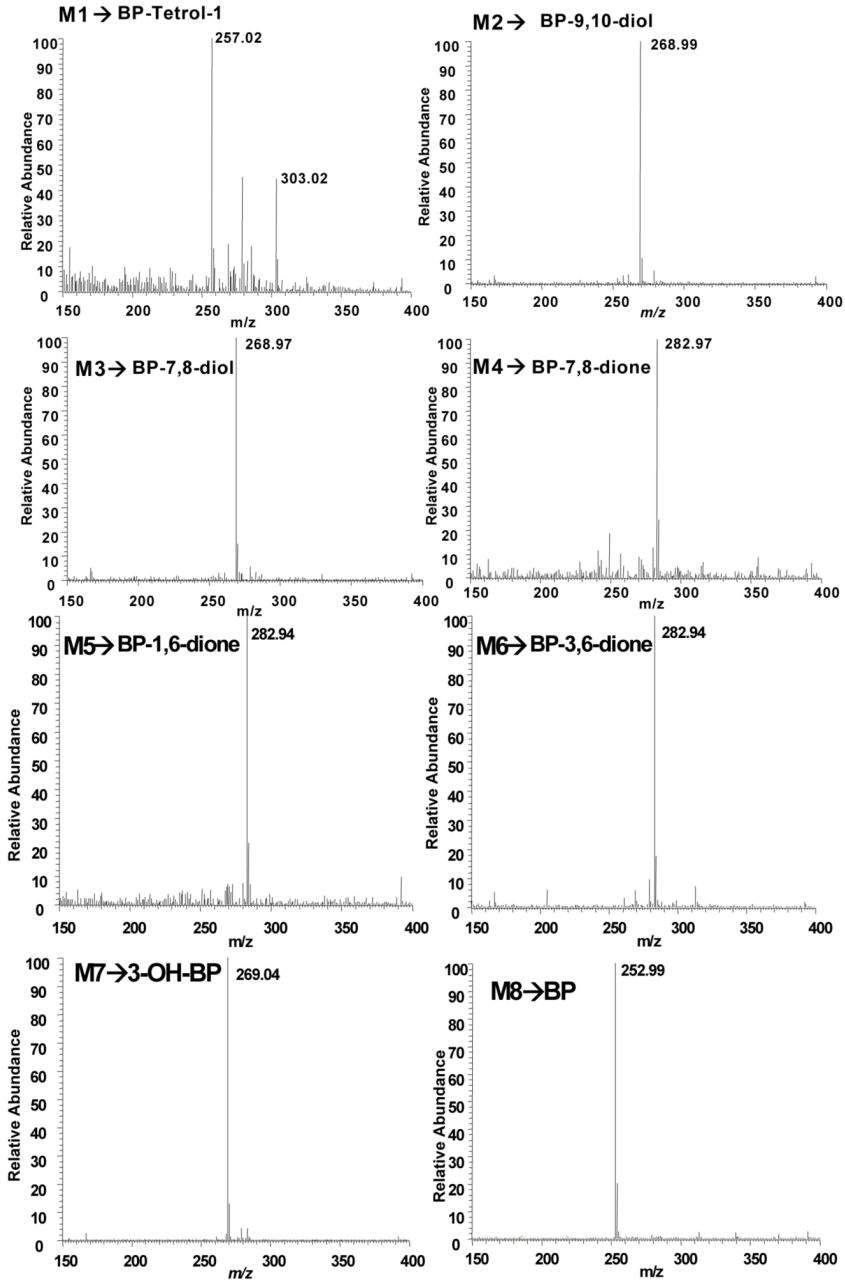

C

Figure 4.

Detection of B[*a*]P-metabolites in parental H358 Cells by LC-MS. Cells (2×10^7) were treated with unlabeled 4 μM unlabeled B[*a*]P for 12 h and the total culture mixture extracted with ethyl acetate. The organic extracts were dried and redissolved in methanol for LC-MS analysis. Chromatographic data were obtained following separation on an ODS column. Mass spectral data were obtained using a Finnigan TSQ Quantum Ultra AM Spectrometer equipped with an APCI source that was operated in the postive ion mode. Analytes were separated by RP-HPLC and the eluant on-line was monitored by the mass spectrometer in the SRM Scan and Q3 full scan modes. The SRM was used to detect the following ion transitions: *m/z* 269 $[M+H-H_2O]^+ \rightarrow$ *m/z* 251 $[M+H-2H_2O]^+$ for B[*a*]P-dihydrodiols (B[a]P-7,8- and 9,10-dihydrodiol);

m/z 269 $[M+H]^+ \rightarrow$ *m/z* 251 $[M+H\text{-}H_2O]^+$ for 3-OH-B[*a*]P; *m/z* 283 $[M+H]^+ \rightarrow$ *m/z* 255 $[M+H\text{-}CO]^+$ for B[*a*]P-quinones (B[*a*]P-7,8-, 1,6-, and 3,6-dione); *m/z* 303 $[M+H\text{-}H_2O]^+ \rightarrow$ *m/z* 285 $[M+H\text{-}2H_2O]^+$ for B[*a*]P-tetraol-1; and *m/z* 253 $[M+H]^+$ for B[*a*]P. Q3 scan was used to obtain mass spectrum of analytes. Panel A, SRMchromatograms of the authentic standards for B[*a*]P-tetraol-1, B[*a*]P-9,10-dihydrodiol, B[*a*]P-7,8-dihydrodiol, B[*a*]P-7,8-dione, B[*a*]P-1,6-dione, B[*a*]P-3,6-dione, 3-OH-B[*a*]P, and B[*a*]P (from the top to the bottom). Panel B, SRM chromatograms of cell organic extract following 12-h B[*a*]P treatment. M1, B[*a*]P-tetraol-1, 15.9 min; M2, B[*a*]P-9,10-dihydrodiol, 20.7 min; M3, B[*a*]P-7,8-dihydrodiol, 35.0 min; M4, B[*a*]P-7,8-dione, 40.4 min; M5, B[*a*]P-1,6-dione, 45.1 min; M6, B[*a*]P-3,6-dione, 47.1 min; M7, 3-OH-B[*a*]P, 59.2 min; M8, B[*a*]P, 78.0 min. Panel C, mass spectra of the B[*a*]P metabolites in H358 cells.

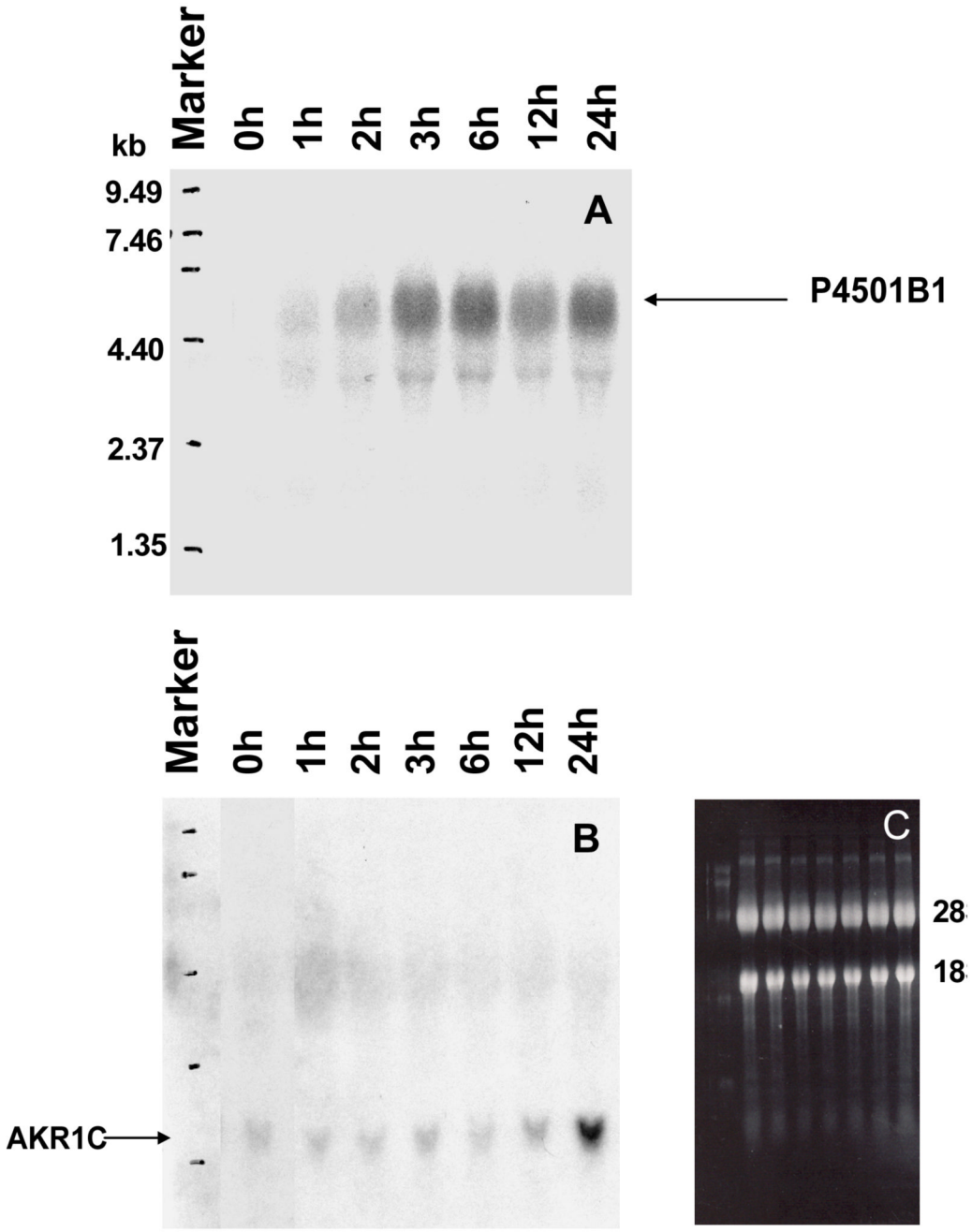

Figure 5.

Time-dependent induction of P4501B1 and AKR1C1 by B[*a*]P in H358 cells. Total cellular RNA was isolated from H358 cells treated with 4 μM B[*a*]P for the indicated time periods and RNA (30 μg) samples obtained were subjected to Northern blotting analysis. The blots were sequentially probed for the expression of P450 1B1 (Panel A) and AKR1C1 (Panel B). Panel C, shows levels of 28S and 18S rRNA following agarose/formaldehyde gel electrophoresis and visualization with ethidium bromide under UV transilluminator at 300 nm to confirm equally loading of each RNA sample.

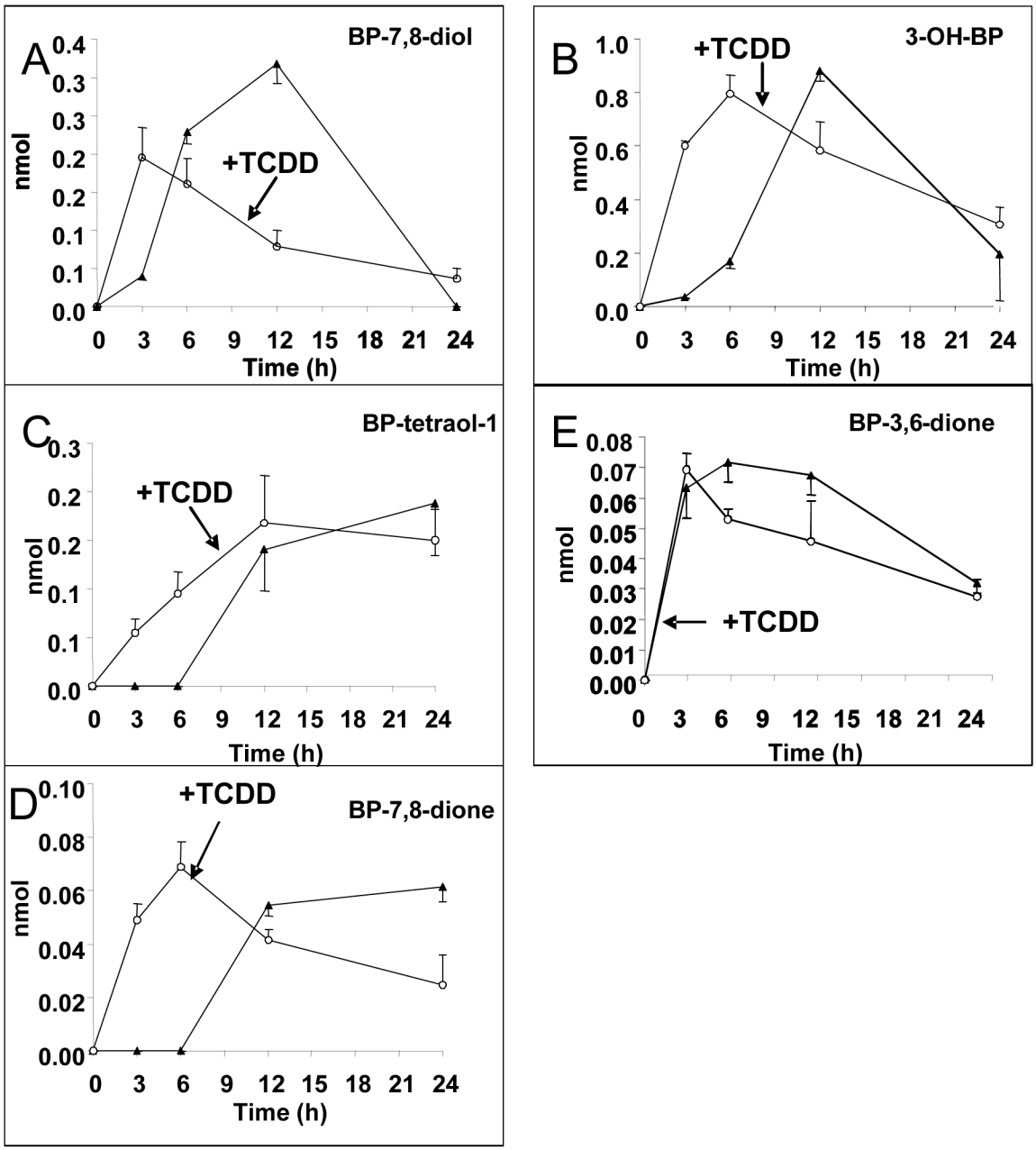

Figure 6.

Time course for B[*a*]P-metabolite formation in the absence and presence of TCDD. B[*a*]P-metabolites were analyzed as described in Figure 2, in parental cells and in H358 cells pre-treated with 10 nM TCDD for 12 h (n =3).